The Study on Water-richness of Thin Limestone Aquifers in North China Coalfields

Situ Lv (lvsitu@163.com)
National Engineering Research Center of Coal Mine Water Hazard Controlling
Longqiang Zhang
China University of Mining and Technology (Beijing)

Article

Keywords:

Posted Date: May 25th, 2022

DOI: https://doi.org/10.21203/rs.3.rs-1630771/v1

Abstract

To obtain the evaluation results that are more in line with the water-richness of thin limestone aquifers for ensuring the safety of coal mine production, dewatering test and hydrochemical analysis were conducted on Benxi thin limestone aquifer to explore and quantify the hydraulic connection between the Ordovician limestone aquifer and the thin limestone aquifer in Benxi formation. Based on the characteristics of water-bearing media, such as aquifer thickness, core recovery, flushing fluid consumption and permeability coefficient, the CRITIC weighting method was used to determine the weight of each factor's influence on the water-richness of thin limestone aquifers, so as to establish the model for evaluating the water-richness of thin limestone aquifer in Benxi formation, and draw the thematic map of the main controlling factors of the aquifers. Then, the information was normalized and superimposed using the multi-source information fusion technology, thereby obtaining the zoning of the aquifer per different water-richness. The evaluation results show that the thin limestone aquifer in Benxi formation can be divided into five areas, i.e. "strong, relatively strong, medium weak, relatively weak and weak " areas. With a stronger hydraulic connection with the Ordovician limestone aquifer, the northwest part of the research area has a greater water-richness than the southeast part, which was verified by the pumping test carried out in the study area.

Introduction

With a stronger development intensity of coal resources, the coal resources in the shallow and upper coal seams of North China coalfields have gradually become insufficient, which makes it an inevitable trend to exploit coal resources in the deep and lower coal seams.[1,2] The increase of the mining depth has also enlarged the possibility of coal mine water disasters during the mining process. The water-richness of the main aquifer in the mining area is one of the important factors that determine the occurrence of coal mine water disasters.[3,4] If the main aquifer in the mining area has a weak water-richness, coal mine water disasters will not happen in general cases; on the contrary, if there are water-rich aquifers in the mining area, coal mine water disasters may occur. Currently, there are primarily two methods to evaluate the water-richness of aquifers.[5–8] One is the water-richness index (WI) method proposed based on GIS.[9] This method analyzes the water-richness of aquifers according to the geological data revealed by borehole survey and the hydrogeological characteristics of the study area. The other is to divide the aquifer into different rock zones by the geophysical survey method, and mathematically evaluate the aquifer's water-richness.[10–12]

With Xingtai Mining Area in Hebei Province of China as the case, exploitation has been successively carried out on the lower coal groups (No.7 and No.9 coal seams) in Gequan Mine, Dongpang Mine, Xingtai Mine etc. However, water inrush with thin limestone aquifers as the water source have occurred many times. Water inrush with limestone water in the Benxi thin layer as the water source occurred twice during the mining of No.9 coal seam in the East Well of Gequan Mine. In fact, since the recharge of thin limestone aquifers varies greatly in the mining area, the water-richness of thin limestone aquifers is

comprehensively influenced by the recharge intensity of the lower Ordovician limestone aquifer and the features of water-bearing media. Hence, it is of great significance to evaluate the water-richness of thin limestone aquifers based on the recharge of Ordovician limestone aquifer and the features of water-bearing media.

Based on the Water-richness Index Method, the dewatering test and hydrochemical analysis were conducted to obtain the recharge of the Ordovician limestone aquifer to thin limestone aquifers.[13,14] The water level data obtained at each observation well at the time of stable dewatering was compared with the initial water level data at the beginning of the dewatering test, and the difference between them can reveal the recharge of the Ordovician limestone aquifer to thin limestone aquifers at the observation well. Due to the particularity of the water-richness of thin limestone aquifers, the water-richness evaluation model of thin limestone aquifers established based on a comprehensive consideration of the Ordovician limestone aquifer's recharge to thin limestone aquifers and the features of water-bearing media can reflect the water-rich zoning of thin limestone aquifers more accurately.

Material And Methods

Study area.

The study area is located in the central part of Xingtai Mining Area (Fig. 1). The coalfield in this area is the Carboniferous-Permian concealed coalfield, and the surface of the study area is all covered by Cenozoic strata.

According to the borehole and roadway surveys, the strata developed in the mining field rank from old to new as follows: Majiagou Formation and Fengfeng Formation of the middle Ordovician system, the middle Benxi Formation and upper Taiyuan Formation of the Carboniferous system, the Lower Shanxi Formation, Lower Shihezi Formation and upper Shihezi Formation of the Permian system, and the Quaternary system. The Quaternary pore aquifer, Permian sandstone fissure aquifer, Carboniferous thin limestone fissure karst aquifer and Ordovician limestone fissure karst aquifer have deposited in the study area. Taiyuan Formation is the main coal-bearing stratum, where No.9 coal seam, with good stability, is one of the main minable coal seams. No.9 coal seam is relatively close to the underlying confined aquifer, with an average distance of about 15m. The underlying confined aquifer, the Benxi formation thin limestone fissure karst confined aquifer, is the research object in this study. There are great differences between different parts of the aquifer in terms of water-richness, karst and fissure are relatively developed in some parts, which are strongly hydraulically connected with the lower Ordovician limestone aquifer, posing a major threat to the mining of No.9 coal seam.

Data.

Aquifer thickness. The thickness of aquifers is one of the important factors influencing the water-richness of aquifers (Fig. 2a). Under normal circumstances, the thicker the aquifer, the greater the water content in the aquifer of unit thickness.

Permeability coefficient. as a significant hydrogeological parameter, is a commonly used index to indicate the permeability of rock strata (Fig. 2b). Permeability coefficient is not only determined by the properties of rock, e.g. particle size, composition, grain arrangement, filling condition, property and development degree of fractures etc., but is also related to the physical properties of fluid such as volume weight and viscosity. When the physical properties of regional groundwater are similar, the greater the permeability coefficient, the stronger the permeability of rock stratum. Given the same physical properties of groundwater in this area, the greater the permeability coefficient, the stronger the permeability of rock strata.

Flushing fluid consumption. Flushing fluid consumption is an important index indicating hydraulic properties of rock strata (Fig. 2c). Flushing fluid not only plays the function of cleaning and lubrication. The variation of flushing fluid consumption represents the lithology and permeability of rock strata. During geological drilling, flushing fluid consumption should be observed in real time. If flushing fluid consumption changes all of a sudden, the permeability of rock strata has changed. Hence, it is of great significance to study the water-richness of aquifers with flushing fluid consumption as one of the influencing factors.

Water level difference. The variation of water level elevation at the observation well during the underground dewatering test is one of the important indices to indicate the recharge intensity of the aquifer in the current area. If the water level at the observation well does not vary drastically during throughout the test, it means that the recharge conditions are favorable in this area, and when the coal mine water disaster occurs, there will be a large amount of water and the disaster will last for a long time; a drastic variation of the water level at the observation well implies poor recharge conditions in this area, which indicates that even if a coal mine water disaster occurs, the losses will be comparatively small (Fig. 2d).

Core recovery. Core recovery refers to the ratio of the total length of the core directly obtained in the borehole (with the length of broken core and weak mud deducted) to the drilling depth (Fig. 2e). It is stipulated that when calculating the core length, only hard and complete cores with a diameter of greater than 10cm should be calculated. Core recovery is a quality index to represent the integrity of rock mass. The lower the core recovery, the more smashed the rock is and the better its connectivity is.

Hydrochemical properties. During the dewatering test, the water in the target aquifer was sampled for the regular hydrogeologic analysis every 24 hours. The hydrochemical properties of groundwater in the discharge aquifer of the mining area and its hydraulic connections with the Ordovician limestone aquifer were explored and analyzed based on the change of the content of main ions in the water.

Methods

CRITIC Weight Method

In this study, the CRITIC weight method was used to determine the weight of each influencing factor on the water-richness of aquifers.[15] Compared with the entropy weight method and the standard deviation method, the CRITIC weight method gives consideration to both the variability and conflict of indices, which, to a great extent, avoids the weight distortion caused by only considering the degree of confusion among indices.[16,17] If the standard deviation between the indices is relatively large, these indices are highly variable and the index weight is comparatively high as well. If the correlation between the indices is weak, it means that these indices strongly conflict with each other, and the index weight is low. The CRITIC weighting model was established in the following specific steps:

Establish the evaluation index matrix. m evaluation indexes were given for n influencing factors. r_{ij} represents the j-th evaluation index of the i-th factor, and the evaluation index matrix was expressed as:

$$R_{nm} = \begin{bmatrix} r_{11} & \cdots & r_{1m} \\ \vdots & \ddots & \vdots \\ r_{n1} & \cdots & r_{nm} \end{bmatrix}$$

Calculate the variability of evaluation indices. The variability of the j-th evaluation index was denoted by the standard deviation:

$$E\left(r_j\right) = \frac{1}{n}\sum_{i=1}^{n} r_{ij}$$

$$\sigma_j = \sqrt{\frac{\sum_{i=1}^{n}(r_{ij} - E\left(r_j\right))^2}{n-1}}$$

Where, $E\left(r_j\right)$ stands for the mean of the j-th evaluation index; σ_j represents the standard deviation of the j-th evaluation index.

Calculate the conflict between evaluation indices. The conflict between the j_1-th and the j_2-th factors was expressed by the Pearson Correlation Coefficient (PCC):

$$\rho_{j_1 j_2} = \frac{Cov(j_1, j_2)}{\sigma_{j_1}\sigma_{j_2}} = \frac{E\left(r_{j_1} \bullet r_{j_2}\right) - E\left(r_{j_1}\right)E\left(r_{j_2}\right)}{\sqrt{E\left({r_{j_1}}^2\right) - E^2\left(r_{j_1}\right)}\sqrt{E\left({r_{j_2}}^2\right) - E^2\left(r_{j_2}\right)}}$$

$$R_{j_1} = \sum_{j_2}^{m} (1 - \rho_{j_1 j_2})$$

Where, $\rho_{j_1 j_2}$ refers to the correlation coefficient between evaluation indices j_1 and j_2; R_{j_1} denotes the conflict of the j_1-th evaluation index; $Cov(j_1, j_2)$ stands for the covariance between two evaluation indices.

Calculate the information quantity of evaluation indices. The information quantity i_j of the j-th evaluation index was expressed as follows:

$$I_j = \sigma_j \bullet R_j$$

Calculate the weight of evaluation indices. The weight W_j of the j-th index factor was expressed as follows:

$$W_j = {I_j}/{\sum_{j=1}^{m} I_j}$$

Data Normalization Method

To eliminate the influences of evaluation indices in different dimensions on the evaluation results, the data must be normalized. The maximum (Eq. 1) or minimum (Eq. 2) method was used to normalize data about the evaluation indices. The maximum method was applied to normalize the influencing factors positively correlated with the water-richness of aquifers, and the minimum method was used to process the influencing factors negatively related to the water-richness of aquifers.

$$Y_i = \frac{y_i - y_{min}}{y_{max} - y_{min}}$$

1

$$Y_i = \frac{y_{max} - y_i}{y_{max} - y_{min}}$$

2

Where, Y_i is the index value of the influencing factor nondimensionalized at point i; y_i denotes the quantified index value of the influencing factor at point i; y_{max} represents the maximum quantified index value of the influencing factor in the study area; y_{min} stands for the minimum quantified index value of the influencing factor in the study area.

Water-richness Index Method

The water-richness pattern and distribution of aquifers are controlled by various factors, with a complicated control mechanism, diverse combination types and influencing conditions. Therefore, it is irrational to determine the water-richness of aquifers in the study area based on a single influencing factor. Based on the multi-source data fusion technology, the water-richness index (WI) method fuses multiple factors that influence the water-richness of aquifers, calculates the weight of each influencing factor, and superposes the constructed thematic maps of evaluation indices to obtain the WI index of aquifer of each evaluation unit in this study area. Natural Jenks, the standard classification method in ArcGIS, was then used to divide all the WI index data into 5 grades, namely weak, relatively weak, medium, relatively strong and strong. The measured data about the specific yield and water inrush points in the target aquifer in the study area were verified in the water-richness zoning map to finally gain the water-richness evaluation model of the target aquifer in the study area.

$$WI = \sum_{i=1}^{m} W_i f_i(x, y)$$

Where, WI is the water-richness index of the aquifer; W_i denotes the weight of influencing factors; $f_i(x, y)$ refers to the single-factor influencing value function; (x, y) represents the geographic coordinates.

Results

Dewatering Test Results

The figure shows the positions of water level observation wells in the dewatering test (Fig. 3). During the dewatering, the water level varied greatly from one observation well to another.

As shown in the variation curve of water level(Fig. 4), at the initial stage of the dewatering test, the water levels at B33, G4 and G10 did not change obviously, while the water levels at the other observation wells all declined. At the end of the test conducted on the first day, the water level at each observation well remained basically stable, and the water levels at different observation wells were greatly inconsistent. In the dewatering test, the water levels at B33, G4 and G10 did not change apparently, but the water levels at the other observation wells changed significantly, with the water level at G6 reaching 96.6m. According to the positions of observation wells and the variation of water levels, the northwest fault zone in the study area is the main channel to recharge the Ordovician limestone aquifer. Since the Ordovician limestone

aquifer is rich in water and strongly hydraulically connected with the Benxi limestone aquifer, the water levels at B33, G10 and G4 did not experience significant change when the water discharge remained steady. Nonetheless, the water levels at G1, G3 and G6 varied remarkably because the runoff conditions of these observation wells were not smooth and they were weakly supplied by Ordovician limestone due to water-blocking faults.

The triangular rhombic hydrogeologic diagram (PiPer diagram) was drawn based on the molar concentration of main ions in water. The molar concentration of anions and cations of each water sample was projected onto the rhombic diagram (Fig. 5), and the hydrogeologic diagram was drawn based on the concentration of main ions in all water samples collected during the dewatering test (Table 1). The different distribution areas of the sample points projected onto the rhombic diagram reflect different hydrochemical types of water samples collected from different aquifers and those from the same aquifer. As shown in the figure, all the sample points fall in the middle-left part of the rhombic diagram in a concentrated way. The point of water sample collected from the Ordovician limestone aquifer at the top of the diagram overlaps with that of water sample collected from the Benxi limestone aquifer. During the dewatering test, the Ordovician limestone aquifer supplies the Benxi aquifer, which is why the samples are similar in hydrogeologic type.

Table 1. Statistical result of hydrochemical indexes for groundwater samples.

Sample	PH	Na+	Ca2+	Mg2+	Cl⁻	SO42⁻	CO32⁻	HCO3⁻	TDS
		mg/L	mg/L	mg/L	mg/L	mg/L	mg/L	mg/L	mg/L
01#	7.64	18.39	59.32	15.07	11.34	48.03		224.54	376.71
05#	7.87	15.63	62.52	16.53	11.34	48.03		234.31	388.36
09#	7.84	18.39	57.72	17.5	12.76	40.35		239.19	385.93
13#	7.58	20.23	67.33	22.48	14.18	34.58		280.68	439.5
16#	7.91	24.83	64.93	17.99	18.44	40.35		270.92	437.49
19#	7.81	20.23	66.53	15.07	11.34	38.42		263.59	415.21
23#	8.02	24.83	60.12	17.99	18.44	40.35		256.27	418.24
Ordovician	8.15	11.95	52.91	17.01	9.93	44.19	2.4	175.73	321.33

The dewatering test and hydrochemical analysis results show a hydraulic connection between the Benxi limestone aquifer and the Ordovician limestone aquifer. Water in the Ordovician limestone aquifer mainly supplies the Benxi limestone aquifer through the fault zone in the northwest of the study area, so the water levels at B33, G4 and G10 did not change significantly during the dewatering test. However, the water blocking effect of SF2, SF1 and Nf101 faults led to an observably variation of the water levels at G1, G3 and G6. The recharge intensity of the Ordovician limestone aquifer in the study area gradually weakens from north to south, with the highest recharge intensity in the northwest fault zone and the north

border area, and the recharge intensity in the central and south parts is weakened due to the water blocking effect of some faults, especially in the south part where the recharge intensity is extremely weak due to the obstruction of SF2, SF1 and Nf101 faults.

Weight Calculation Results

The table shows the weight of different influencing factors calculated using the CRITIC weight method (Table 2).

Table 2. Weight calculation of CRITIC.

Influencing factor	Variability	Conflict	Information quantity	Weight
Aquifer thickness	0.184	4.067	0.749	0.182
Core recovery	0.181	3.592	0.649	0.158
Flushing fluid consumption	0.285	3.193	1.116	0.271
Permeability coefficient	0.27	3.164	0.855	0.208
Water level elevation	0.219	3.396	0.744	0.181

Results of the WI Evaluation Model

According to the weight of different influencing factors calculated above, the thematic maps of the 5 evaluation indices were superposed and fused to obtain the WI index of aquifer of each evaluation unit in this study area.

$$WI = \sum_{i=1}^{m} W_i f_i(x, y) = 0.182 \bullet f_1(x, y) + 0.182 \bullet f_1(x, y) +$$

$$0.158 \bullet f_2(x, y) + 0.271 \bullet f_3(x, y) + 0.208 \bullet f_4(x, y) + 0.181 \bullet f_5(x, y)$$

Then, Natural Jenks, the standard classification method in ArcGIS, was applied to divide all the WI index data into 5 grades, weak, relatively weak, medium, relatively strong and strong. GIS was used to draw the water-richness zoning map of the Benxi limestone aquifer in the study area. The 4 sets of data about the specific yield and 2 sets of data about water inrush points measured in the study area was verified in the water-richness zone map (Table 3).[18,19] All the bores with a measured specific yield of greater than 0.5(L/s·m) are located in the strong water-richness area, bores with a measured specific yield of greater than 0.1(L/s·m) are located in the medium weak area, those with a measured specific yield of smaller than 0.1(L/s·m) are located in the weak area, and all the water inrush points are situated in the relatively strong area. It verifies that the water-richness zone of thin limestone aquifers in this study is accurate and reliable.

Table 3. Information on relevant bores in the study area.

Bore	Specific yield (L/s·m)	Bore	Specific yield (L/s·m)
B35	2.233	B41	0.175
B33	0.667	B42	0.0058

As shown in the figure, the water-richness of the Benxi limestone aquifer in the East Well of Gequan Mine weakens from the northwest to the southeast. Different water-richness areas are distributed unevenly in the aquifer. The strong and relatively strong water-richness areas are mainly concentrated in the northwest part of the study area, the areas with medium weak water-richness are distributed along the southwest-northeast direction in the form of strips, while the rest parts are classified as relatively weak and weak water-richness areas (Fig. 6).

Conclusion

(1) The upper part of Ordovician limestone in Xingtai mining area is generally covered with one or more thin limestone aquifers. Due to the development of geological structures and fissures in some areas, there is a strong hydraulic connection between the thin limestone and the lower Ordovician limestone aquifer. Consequently, the thin limestone aquifers in the study area are featured by relatively strong water-richness, which poses a threat to mining.

(2) Compared with the other types of aquifers, the water-richness of thin limestone aquifers is more affected by the recharge intensity. Water inrush is less likely to occur in thin limestone aquifers when the recharge intensity is weak. However, in areas with strong recharge intensity, there is a very high probability of water inrush accidents in thin limestone aquifers with continuous recharge. Hence, recharge intensity is a factor that should not be ignored in the water-rich evaluation of thin limestone aquifers.

(3) Based on the dewatering test and hydrochemical analysis results of the East Well of Gequan Mine, there is a strong hydraulic connection between the Benxi limestone aquifer and the Ordovician limestone aquifer in the study area, and water from the Ordovician limestone aquifer supplies the Benxi limestone aquifer through the fault zone in the northwest of the study area. However, the water blocking effect of SF2, SF1 and Nf101 faults results in great differences between the recharge intensity of different parts of the study area, with the recharge intensity of the north part being significantly stronger than that of the south part.

(4) The recharge intensity of the lower Ordovician limestone aquifer, the thickness of the aquifer, core recovery, flushing fluid consumption and permeability coefficient were used as the water-richness evaluation indices. The CRITIC weight method was applied to determine the weight of main controlling factors on the water-richness and establish the water-richness evaluation model. The model was verified based on the specific yield obtained in previous dewatering tests and the positions of water inrush points in the Benxi limestone aquifer, the results of which implied high accuracy of the water-richness evaluation model. The water-richness of the Benxi limestone aquifer in the East Well of Gequan Mine weakens from

the northwest to the southeast, with the relatively strong water-rich zones concentrated in the northwest fault zone and the north boundary, while zones in the southeast and south parts of the study area having relatively weak water-richness.

Declarations

Author contributions statement

SL contributed to conceptualization, methodology, software, formal analysis, and writing-original draft and editing. LZ contributed to methodology and editing. All authors reviewed the manuscript.

Competing interests

The authors declare no competing interests.

Data availability

The datasets generated and analysed during the current study are not publicly available due keep secret but are available from the corresponding author on reasonable request.

References

1. Xie, H.-P. *et al.* Research and consideration on deep coal mining and critical mining depth. Meitan Xuebao/Journal of the China Coal Society **37**, 535–542 (2012).
2. Li, W. P. *et al.* An Improved Vulnerability Assessment Model for Floor Water Bursting from a Confined Aquifer Based on the Water Inrush Coefficient Method. Mine Water Environ. **37**, 196–204, doi:10.1007/s10230-017-0463-3 (2018).
3. Dong, D. L., Sun, W. J. & Xi, S. Water-inrush Assessment Using a GIS-based Bayesian Network for the 12 – 2 Coal Seam of the Kailuan Donghuantuo Coal Mine in China. Mine Water Environ. **31**, 138–146, doi:10.1007/s10230-012-0178-4 (2012).
4. Wang, L. G. A model to risk assessment for mine water inrush. J.Eng.Geol. **9**(**02**), 58–163 (2001).((**in chinese**))
5. Nampak, H., Pradhan, B. & Abd Manap, M. Application of GIS based data driven evidential belief function model to predict groundwater potential zonation. J. Hydrol. **513**, 283–300, doi:10.1016/j.jhydrol.2014.02.053 (2014).
6. Gossel, W., Ebraheem, A. M. & Wycisk, P. A very large scale GIS-based groundwater flow model for the Nubian sandstone aquifer in Eastern Sahara (Egypt, northern Sudan and eastern Libya). Hydrogeol. J. **12**, 698–713, doi:10.1007/s10040-004-0379-4 (2004).

7. Pourghasemi, H. R. & Beheshtirad, M. Assessment of a data-driven evidential belief function model and GIS for groundwater potential mapping in the Koohrang Watershed, Iran. Geocarto Int. **30**, 662–685, doi:10.1080/10106049.2014.966161 (2015).
8. Sherif, M. I. *et al.* Geological and hydrogeochemical controls on radium isotopes in groundwater of the Sinai Peninsula, Egypt. Sci. Total Environ. **613**, 877–885, doi:10.1016/j.scitotenv.2017.09.129 (2018).
9. Wu, Q., Fan, Z.-L., Liu, S.-Q., Zhang, Y.-W. & Sun, W.-J. Water-richness evaluation method of water-filled aquifer based on the principle of information fusion with GIS: Water-richness index method. Meitan Xuebao/Journal of the China Coal Society **36**, 1124–1128 (2011).
10. Yin, H. Y. *et al.* A GIS-based model of potential groundwater yield zonation for a sandstone aquifer in the Juye Coalfield, Shangdong, China. J. Hydrol. **557**, 434–447, doi:10.1016/j.jhydrol.2017.12.043 (2018).
11. Shi, L. Q. e. a. Application of 3D high density technique in detecting the water enrichment of strata. J.Shandong Univ.Sci.Technol.(Nat.Sci.) **27**(**06**), 1–4, doi:https://doi.org/10.16452/j.cnki.sdkjzk.2008.06.006 (2008).
12. Qiu, M., Shi, L., Teng, C. & Han, J. Water-richness evaluation of ordovician limestone based on grey correlation analysis, FDAHP and geophysical exploration. Yanshilixue Yu Gongcheng Xuebao/Chinese Journal of Rock Mechanics and Engineering **35**, 3203–3213, doi:10.13722/j.cnki.jrme.2015.0916 (2016).
13. Zhao, B. X., Lv,Y.G,. Analysis on water conductivity of fault based on pumping test and dewatering test. Safety in Coal Mines **53.1**, 52–62, doi:https://10.13347/j.cnki.mkaq.2022.01.009 (2022).
14. Qiao, Y. *et al.* Characteristics of mine aquifer with complex structure and identification of its hydraulic connection. Meitan Xuebao/Journal of the China Coal Society **46**, 4010–4020, doi:10.13225/j.cnki.jccs.2021.1247 (2021).
15. D. Diakoulaki, G. M., L. Papayannakis,. Determining objective weights in multiple criteria problems: The critic method. Computers & Operations Research **22**, 763–770, doi:https://doi.org/10.1016/0305-0548(94)00059-H. (1995).
16. Xu, C. B., Ke, Y. M., Li, Y. B., Chu, H. & Wu, Y. N. Data-driven configuration optimization of an off-grid wind/PV/hydrogen system based on modified NSGA-II and CRITIC-TOPSIS. Energy Conv. Manag. **215**, 18, doi:10.1016/j.enconman.2020.112892 (2020).
17. Keshavarz Ghorabaee, M., Amiri, M., Zavadskas, E. K. & Antucheviciene, J. ASSESSMENT OF THIRD-PARTY LOGISTICS PROVIDERS USING A CRITIC-WASPAS APPROACH WITH INTERVAL TYPE-2 FUZZY SETS. Transport **32**, 66–78, doi:10.3846/16484142.2017.1282381 (2017).
18. Sun, J. *et al.* Tracing and quantifying contributions of end members to karst water at a coalfield in southwest China. Chemosphere **234**, 777–788, doi:10.1016/j.chemosphere.2019.06.066 (2019).
19. Stevanovic, Z. Karst waters in potable water supply: a global scale overview. Environ. Earth Sci. **78**, 12, doi:10.1007/s12665-019-8670-9 (2019).

Figures

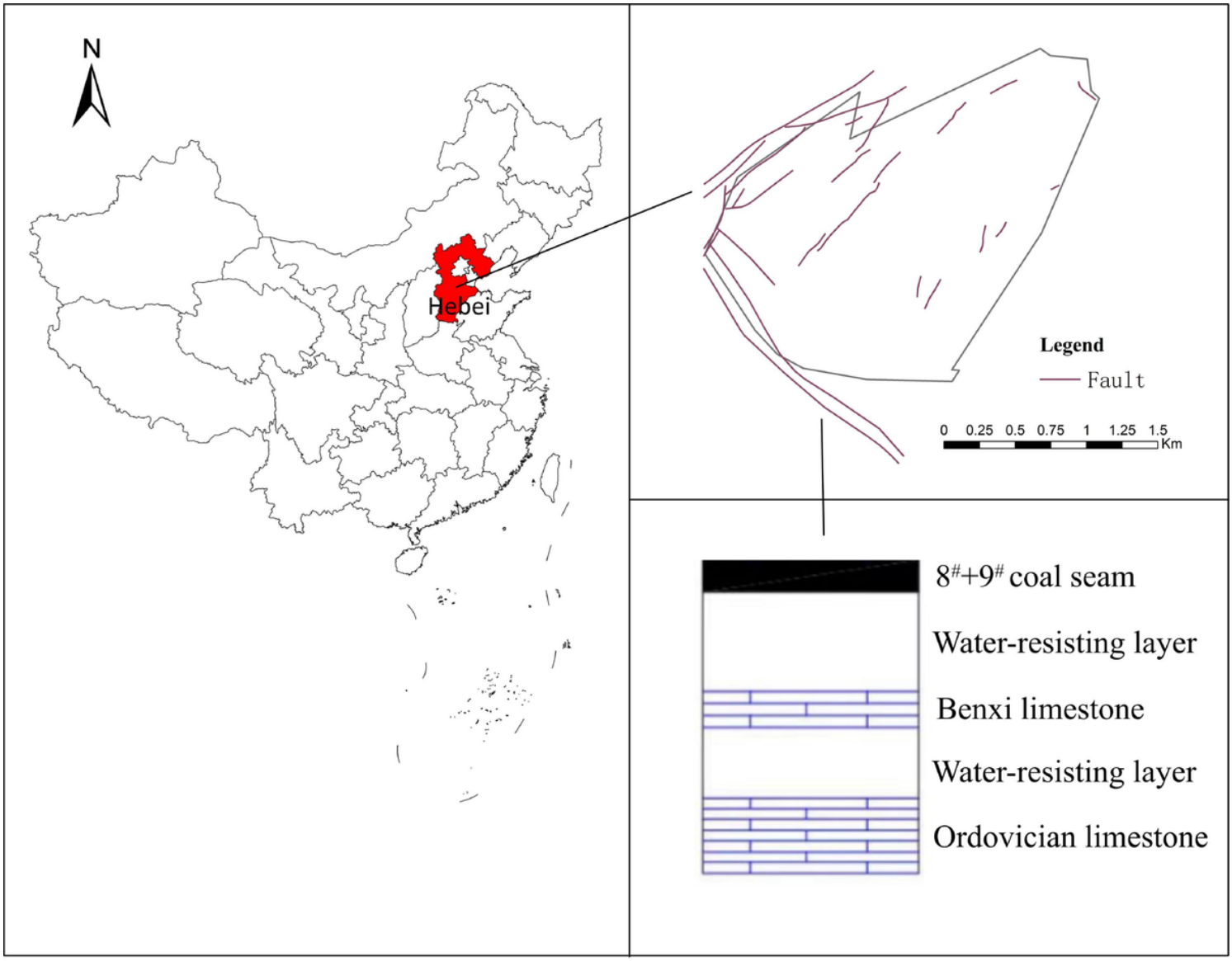

Figure 1

Location and structural geology map

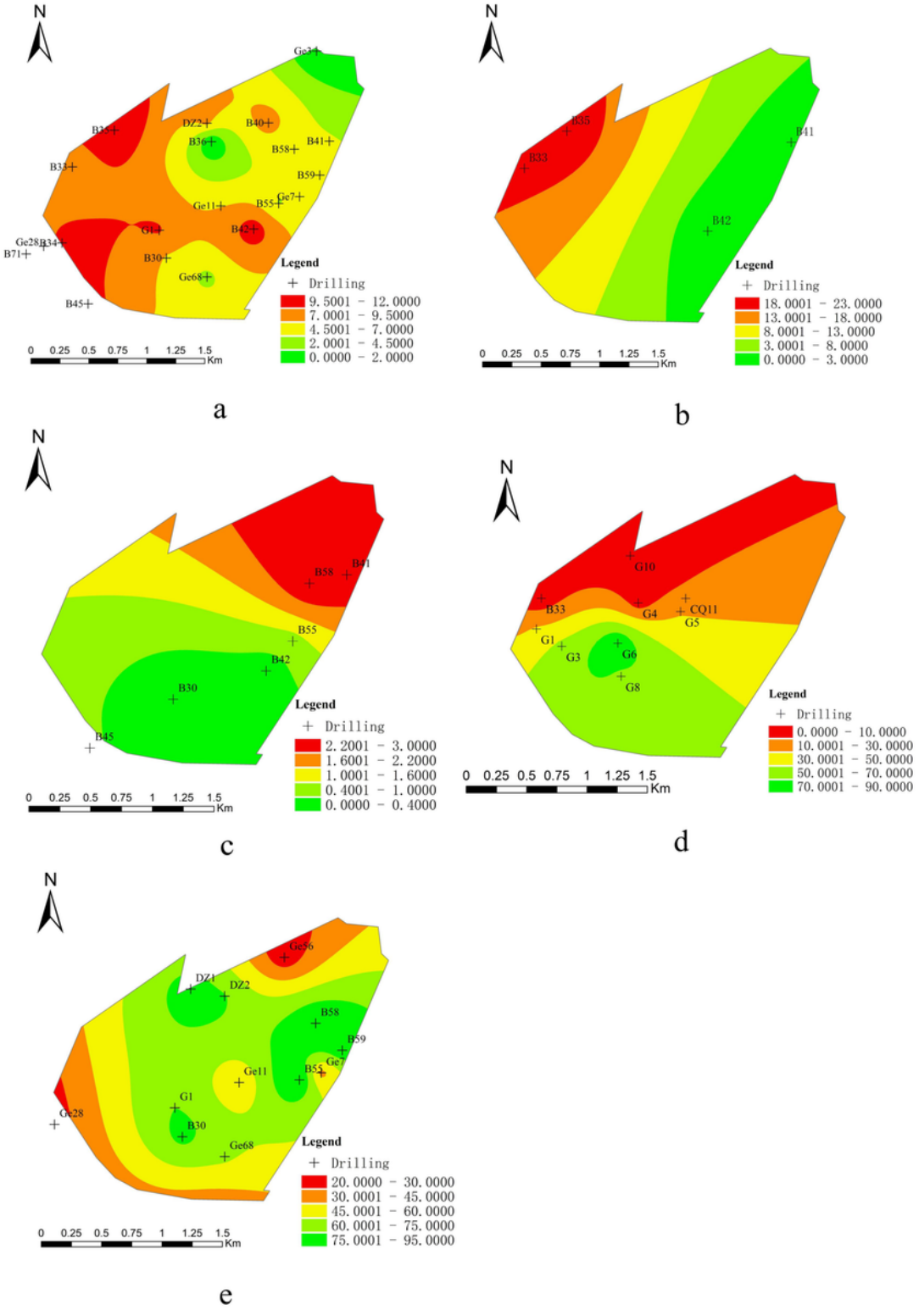

Figure 2

Influence factors of water-richness: (**a**) Aquifer thickness(m), (**b**) Permeability coefficient(m/d), (**c**) Flushing fluid consumption(m3/h), (**d**) Water level difference (m), (**e**) Core recovery(%).

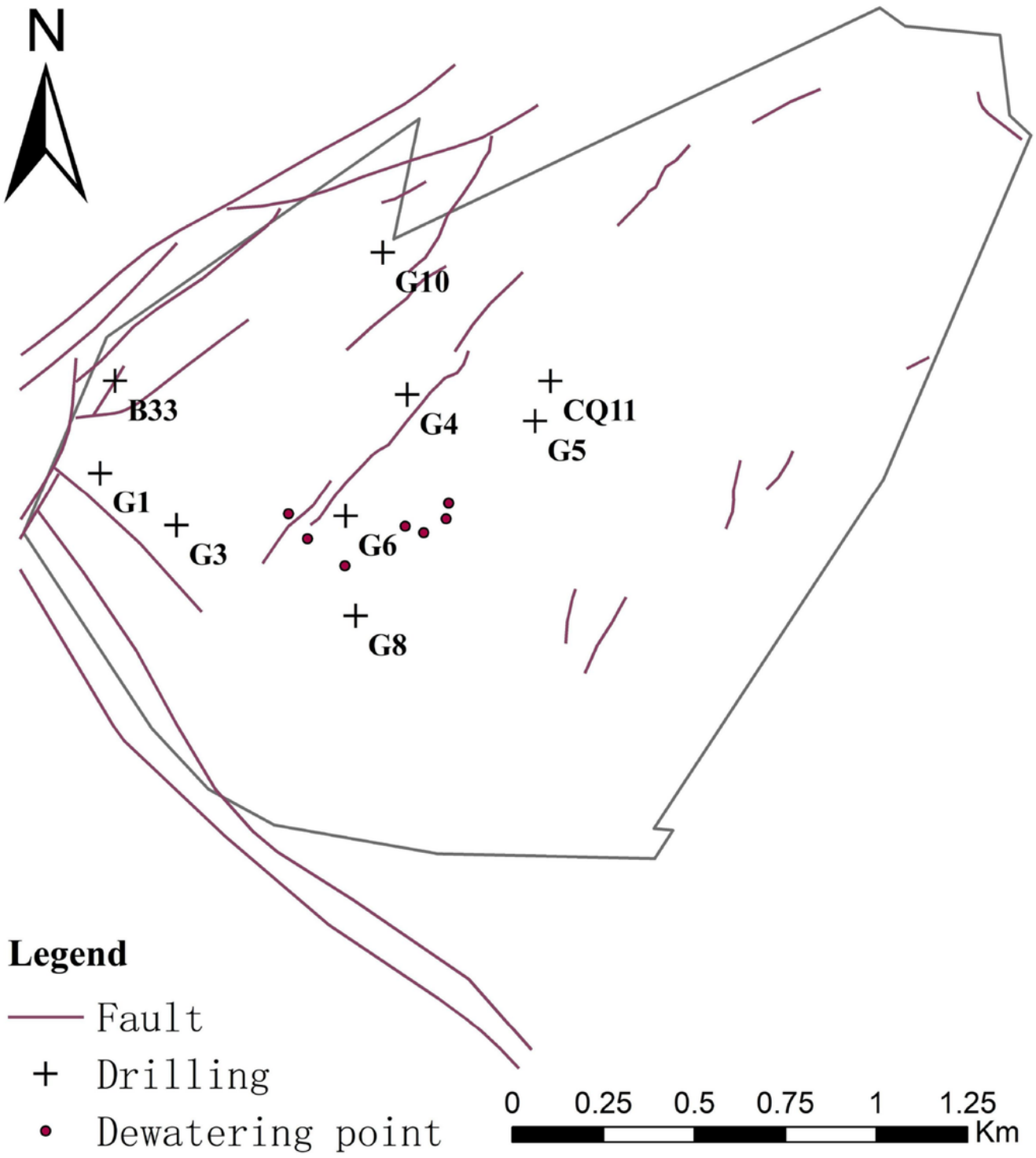

Figure 3

The positions of water level observation wells

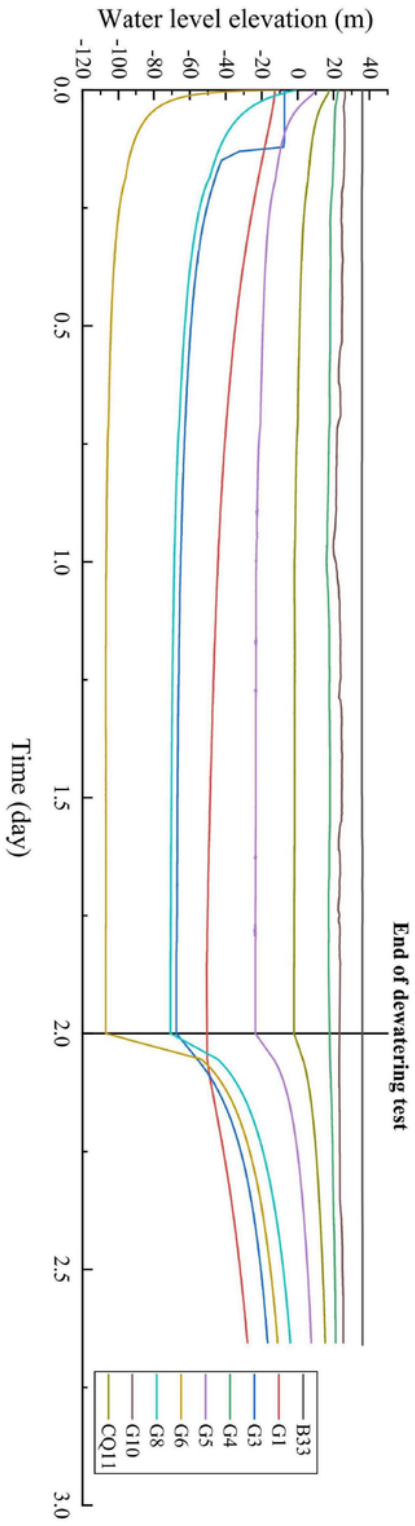

Figure 4

Graph of observed water level changes during the dewatering test.

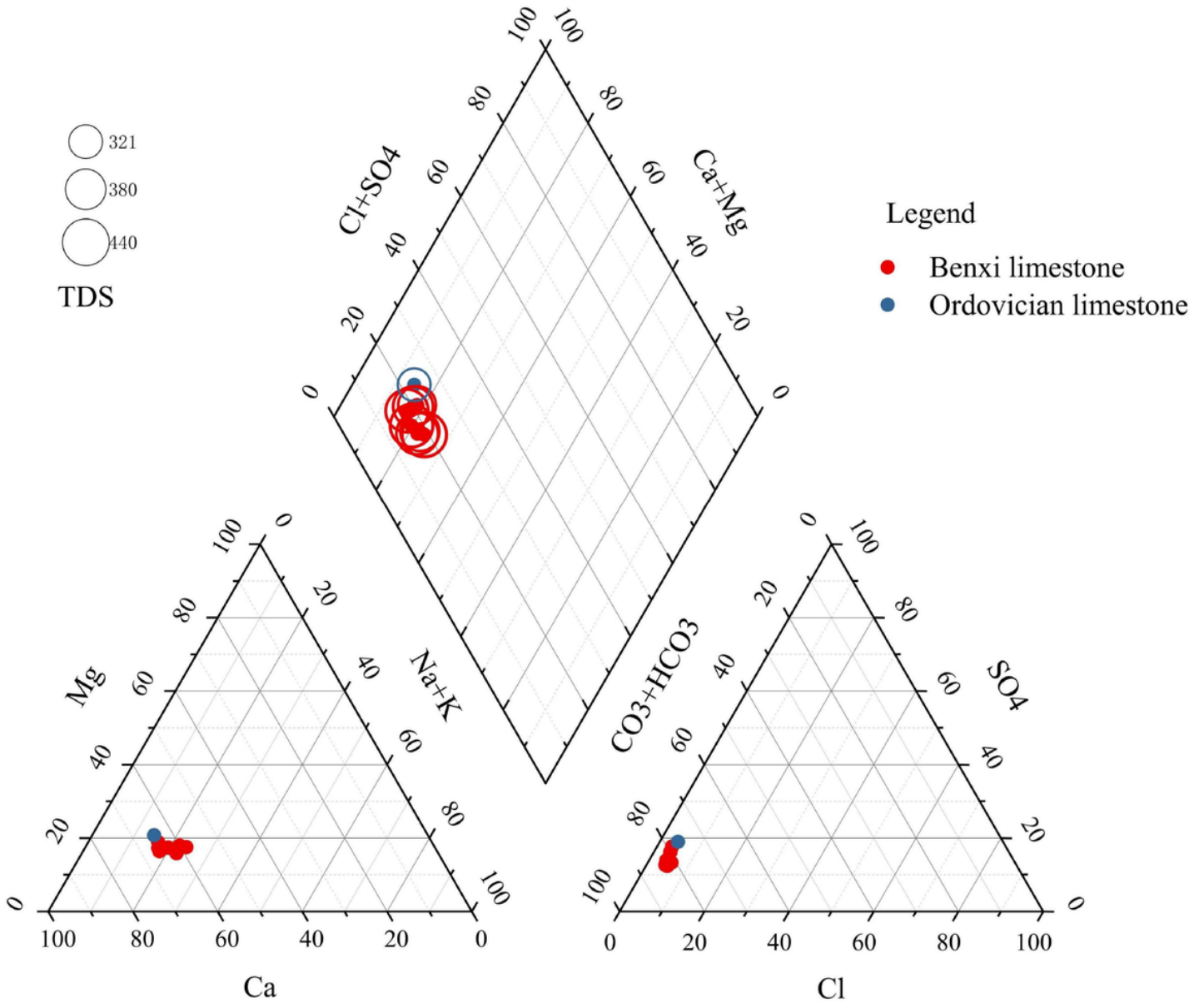

Figure 5

Piper comparison of water samples.

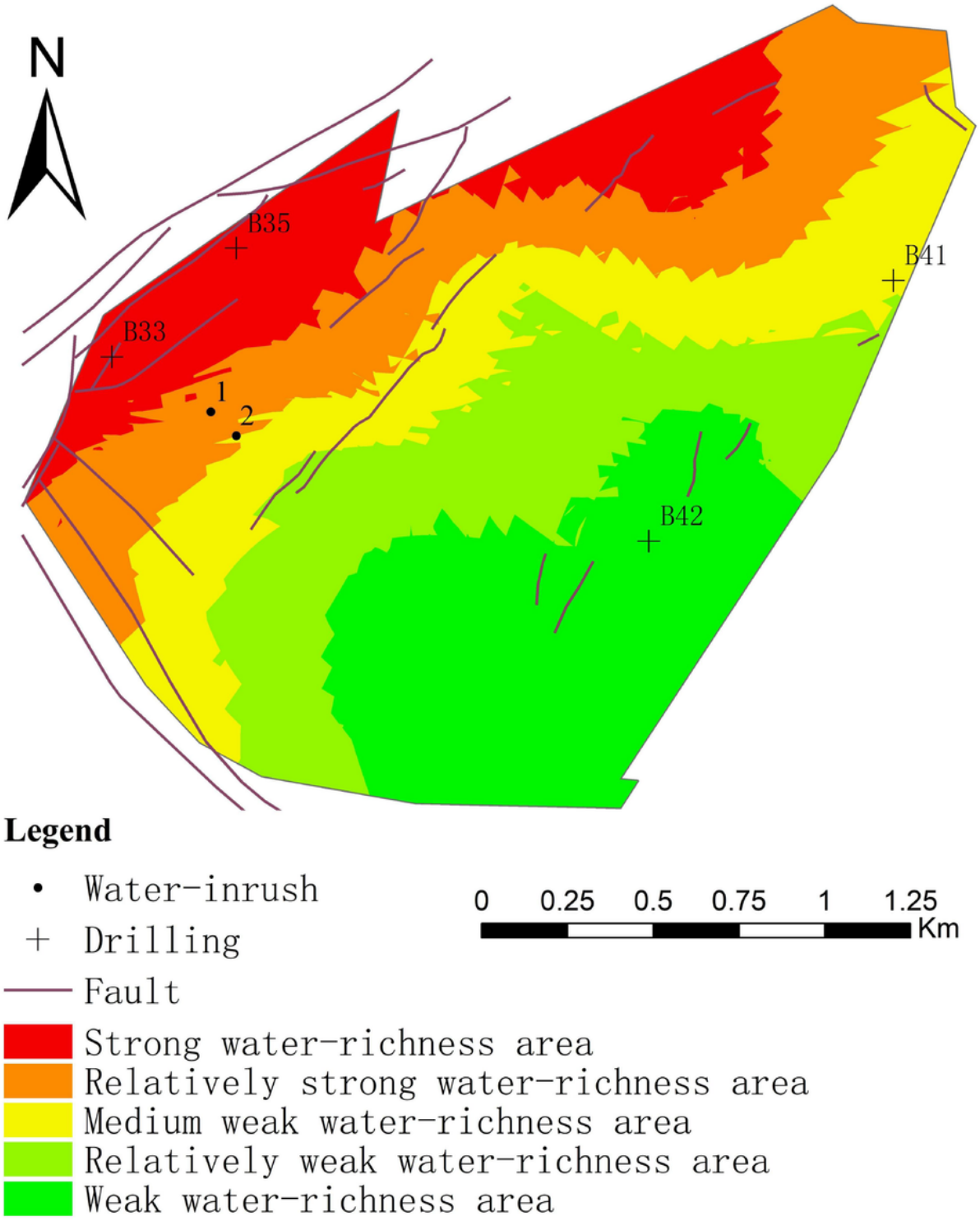

Figure 6

Water-richness zone map of the study area.